remote sensing

MDPI

Article

Integrating Drone Truthing and Functional Classification of Remote Sensing Time Series for Supervised Vegetation Mapping

Giacomo Quattrini [1], Simone Pesaresi [1,*], Nicole Hofmann [1], Adriano Mancini [2] and Simona Casavecchia [1]

[1] Department of Agricultural, Food and Environmental Sciences, D3A, Università Politecnica delle Marche, Via Brecce Bianche 12, 60131 Ancona, Italy; g.quattrini@pm.univpm.it (G.Q.); n.hofmann@univpm.it (N.H.); s.casavecchia@univpm.it (S.C.)

[2] Department of Information Engineering, DII, Università Politecnica delle Marche, Via Brecce Bianche 12, 60131 Ancona, Italy; a.mancini@univpm.it

* Correspondence: s.pesaresi@univpm.it

Abstract: Accurate vegetation mapping is essential for monitoring biodiversity and managing habitats, particularly in the context of increasing environmental pressures and conservation needs. Ground truthing plays a crucial role in ensuring the accuracy of supervised remote sensing maps, as it provides the high-quality reference data needed for model training and validation. However, traditional ground truthing methods are labor-intensive, time-consuming and restricted in spatial coverage, posing challenges for large-scale or complex landscapes. The advent of drone technology offers an efficient and cost-effective solution to these limitations, enabling the rapid collection of high-resolution imagery even in remote or inaccessible areas. This study proposes an approach to enhance the efficiency of supervised vegetation mapping in complex landscapes, integrating Multivariate Functional Principal Component Analysis (MFPCA) applied to the Sentinel-2 time series with drone-based ground truthing. Unlike traditional ground truthing activities, drone truthing enabled the generation of large, spatially balanced reference datasets, which are critical for machine learning classification systems. These datasets improved classification accuracy by ensuring a comprehensive representation of vegetation spectral variability, enabling the classifier to identify the key phenological patterns that best characterize and distinguish different vegetation types across the landscape. The proposed methodology achieves a classification accuracy of 92.59%, significantly exceeding the commonly reported thresholds for habitat mapping. This approach, characterized by its efficiency, repeatability and adaptability, aligns seamlessly with key environmental monitoring and conservation policies, such as the Habitats Directive. By integrating advanced remote sensing with drone-based technologies, it offers a scalable and cost-effective solution to the challenges of biodiversity monitoring, enabling timely updates and supporting effective habitat management in diverse and complex environments.

Keywords: phytosociology; vegetation mapping; remote sensing time series; MFPCA; ground truthing; drone; habitat monitoring

Academic Editor: Dongmei Chen

Received: 4 December 2024
Revised: 14 January 2025
Accepted: 17 January 2025
Published: 18 January 2025

Citation: Quattrini, G.; Pesaresi, S.; Hofmann, N.; Mancini, A.; Casavecchia, S. Integrating Drone Truthing and Functional Classification of Remote Sensing Time Series for Supervised Vegetation Mapping. *Remote Sens.* **2025**, *17*, 330. https://doi.org/10.3390/rs17020330

1. Introduction

The classification and mapping of plant communities and habitats are crucial for biodiversity monitoring and the development of conservation strategies, particularly in Natura 2000 sites across Europe [1,2]. The 92/43/EEC Habitats Directive represents the cornerstone of the European conservation policy, focusing on biodiversity preservation [3]. Within this framework, the phytosociological approach plays a critical role by providing a

structured method for vegetation classification, enabling the identification and diagnosis of natural and semi-natural habitats listed in Annex I of the Directive [4–7]. For this reason, phytosociological mapping is of fundamental importance as it provides detailed spatial information on habitats, helping to identify conservation priorities [8–10].

Today, vegetation phytosociological mapping benefits from the integration of machine learning methods with remote sensing time series [9,11–13]. Platforms like Landsat, MODIS and Sentinel provide multi-temporal, multi-spectral data that capture seasonal variations in spectral reflectance in relation to vegetation phenological stages, which provide key information for distinguishing different vegetation types [14–17]. The supervised classification of multi-spectral time series data using machine learning methods allows for the creation of accurate vegetation and habitat maps [18–22]. Despite these technological advancements, which enhance the accuracy of habitat and vegetation mapping, certain gaps remain [23,24]. Ichter et al. [8,25] report that, while these phytosociological and habitat maps are often highly accurate, they are rarely updated or repeated over time. This lack of continuous, timely mapping limits the maps' utility as a crucial monitoring tool for assessing the habitat conservation status, fragmentation trends or signs of habitat degradation.

One of the primary obstacles to an efficient mapping process, limiting both the production and updating of maps, is no longer the processing and analysis of satellite time series or their classification, but rather the constraints imposed by ground truthing activities [26,27], which are crucial for creating a reference dataset necessary for training and assessing the effectiveness of the classification [28,29]. The success of supervised classification relies fundamentally on the quality of this reference data, which must be exhaustive, spatially balanced and accurately representative of the predefined vegetation classes [30–35]. Generating these data by traditional ground truthing activities (e.g., Braun-Blanquet approach) demands considerable effort, making the comprehensive collection of reference data the main bottleneck in phytosociological supervised mapping [9,36].

To address this challenge, drones offer an efficient and cost-effective solution for enhancing reference data collection through "drone truthing" activities [37–39]. Their ability to access even hard-to-reach areas, combined with the capability to capture high-resolution RGB imagery, provides a powerful tool for identifying dominant and diagnostic plant species at verification sites, even in complex environments [40–42]. Based on this imagery, vegetation categories (plant communities) and habitat types, as defined by Annex I of the Habitat Directive, will be assigned to all of the sites identified in the sampling design.

We assess the effectiveness and suitability of this methodology in Natura 2000 sites within the Furlo Gorge, a mountainous area in central Italy characterized by high vegetation and topographic diversity and complexity.

This study aims to enhance the efficiency of phytosociological vegetation mapping by using the supervised classification of multi-spectral seasonal variations, integrating on-site field verification and drone-based truthing by creating a dense, spatially balanced reference dataset for training and validation, enhancing both the consistency and frequency of mapping efforts.

2. Materials and Methods

In this section, we present the workflow (Figure 1) adopted to produce the vegetation map for the area of interest through a supervised classification of seasonal spectral variations derived from a dense time series of remote sensing data. We began by collecting time series data from the Sentinel-2 satellite, utilizing all available spectral bands. The data for each band were transformed into continuous functions using Generalized Additive Models (GAM). These functions were then analyzed with Functional Data Analysis (FDA), employing a Multivariate Functional Principal Component Analysis (MFPCA). The scores

derived from MFPCA were used as the input for machine learning methods to carry out a supervised functional classification and generate the final map. Reference data, obtained through ground truthing and "drone truthing" activities, were used to train the model and validate its accuracy. Further details are provided in the subsequent sections.

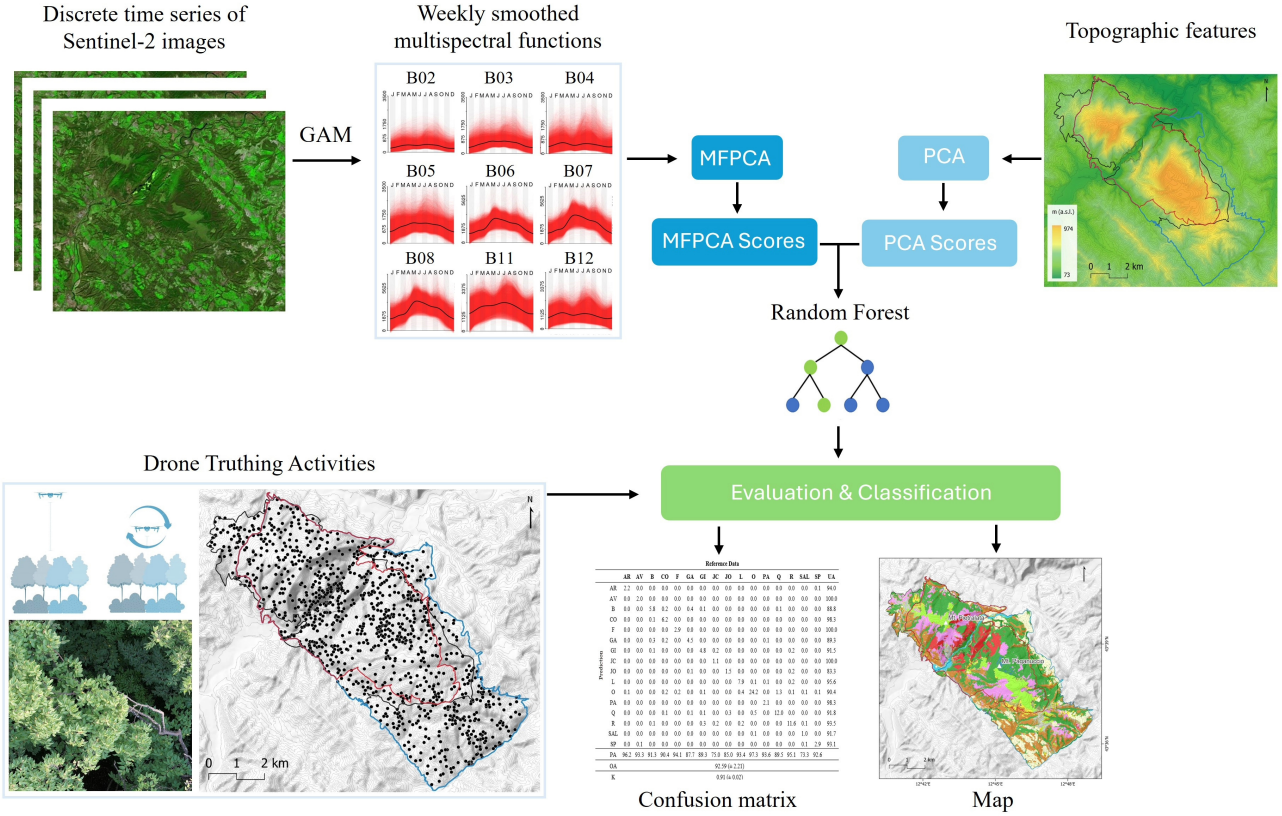

Figure 1. Supervised pipeline to derive plant associations and habitat maps from Sentinel-2 time series using Multivariate Functional Principal Component Analysis and drone truthing activities.

2.1. Study Area

The study area covers 51.95 km^2 and is located along the central Apennine ridge in the Marche Region, Italy (Figure 2). It encompasses territories within the Gola del Furlo State Nature Reserve and the Natura 2000 sites, specifically the Special Protection Area (SPA) "Furlo" (IT5310029) and the Special Area of Conservation (SAC) "Gola del Furlo" (IT5310016). The area features significant topographical variation with predominantly calcareous bedrock. It includes Monte Pietralata (888 m) to the north and Monte Paganuccio (974 m) to the south, divided by a narrow gorge carved by the Candigliano River. The mean annual precipitation in the area ranges from 950 to 1180 mm, and the mean annual temperature varies between 10.5 °C and 13.5 °C. According to the bioclimatic classification by Rivas-Martinez et al. [43], the area belongs to the temperate macro bioclimate with a weak sub-Mediterranean level, which indicates low summer aridity in areas below 600 m in altitude [44]. The vegetative landscape is predominantly characterized by forests and summit meadows.

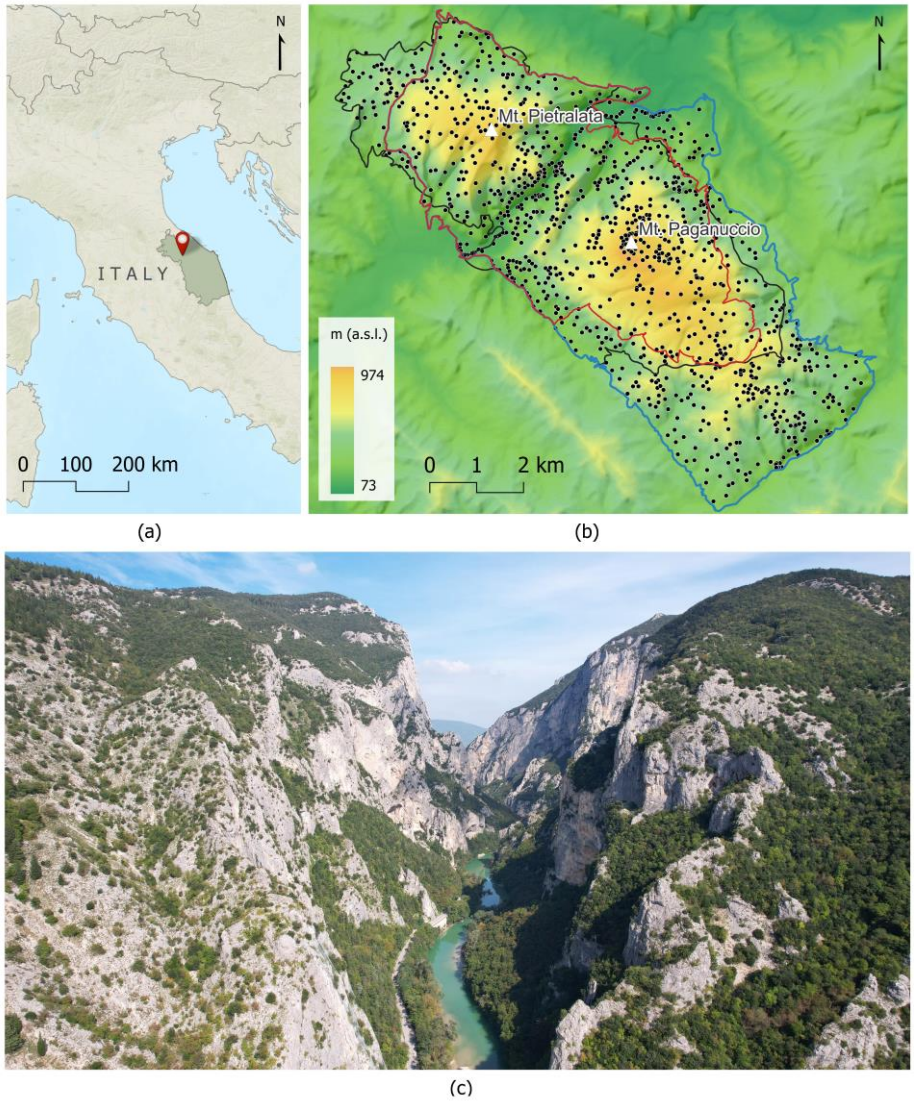

Figure 2. Study area: (**a**) overview of the study area on a regional scale. (**b**) Reference data overlaid on the Digital Elevation Model, marking the boundaries of the Gola del Furlo State Nature Reserve (in black), the Special Protection Area (SPA) "Furlo" (code: IT5310029) (in blue) and the Special Area of Conservation (SAC) "Gola del Furlo" (IT5310016) (in red). (**c**) Entry points to the Furlo Gorge, with Mount Paganuccio to the left and Mount Pietralata to the right.

2.2. Target Classes and Reference Data (Ground Truthing and Drone Truthing)

The target mapping classes, listed in Table 1, represent physiognomic vegetation types based on the dominant plant species and habitats defined by Directive 92/43/EEC. Table A1 provides details on the corresponding plant associations, identified using the Braun-Blanquet method [45]. In most cases, each physiognomic vegetation type corresponds to a single plant association, while some, such as holm oak and black hornbeam forests, encompass multiple associations.

To create a spatially balanced reference dataset, a randomized sampling design was implemented using the R package "spsurvey" (version 5.5.1) [46]. A total of 1,118 points/plots were randomly positioned within the study area (Figure 2b). Each point requires the assignment to one of the vegetation mapping classes from Table 1, based on the most abundant dominant species. Relying solely on field verification to assign mapping classes to each plot would be time-consuming and, occasionally, impractical due to the inaccessibility or hazardous conditions of the locations. To enhance the efficiency of the assignment process, we have introduced a verification method that utilizes high-resolution images

from drone surveys. High-resolution visible imagery was captured using a 20-megapixel camera equipped with a 1-inch CMOS sensor mounted on a DJI Air 2S drone. This drone has a Maximum Takeoff Mass (MTOM) of 595 g, a maximum battery life of 30 min and a GNSS positioning system that ensures a horizontal hovering accuracy ranging from ±0.1 m to ±1.5 m.

The flight operations were manually controlled for the navigation to the verification sites and to reach them at a vertical distance of about 5 m from the canopy, using the drone's obstacle detection sensors. Once in position, the drone hovered and took five photos: one nadir view and four shots in the cardinal directions. Preliminary tests have shown that these five high-resolution photos allow botanists to identify the most abundant species and assign the site to one of the target vegetation categories for the mapping of Table 1. Subsequently, the drone is raised by about 20 m to take a wider panoramic shot from approximately 25 m above the canopy, providing a sixth photo with an overall view of the area (Figure 3).

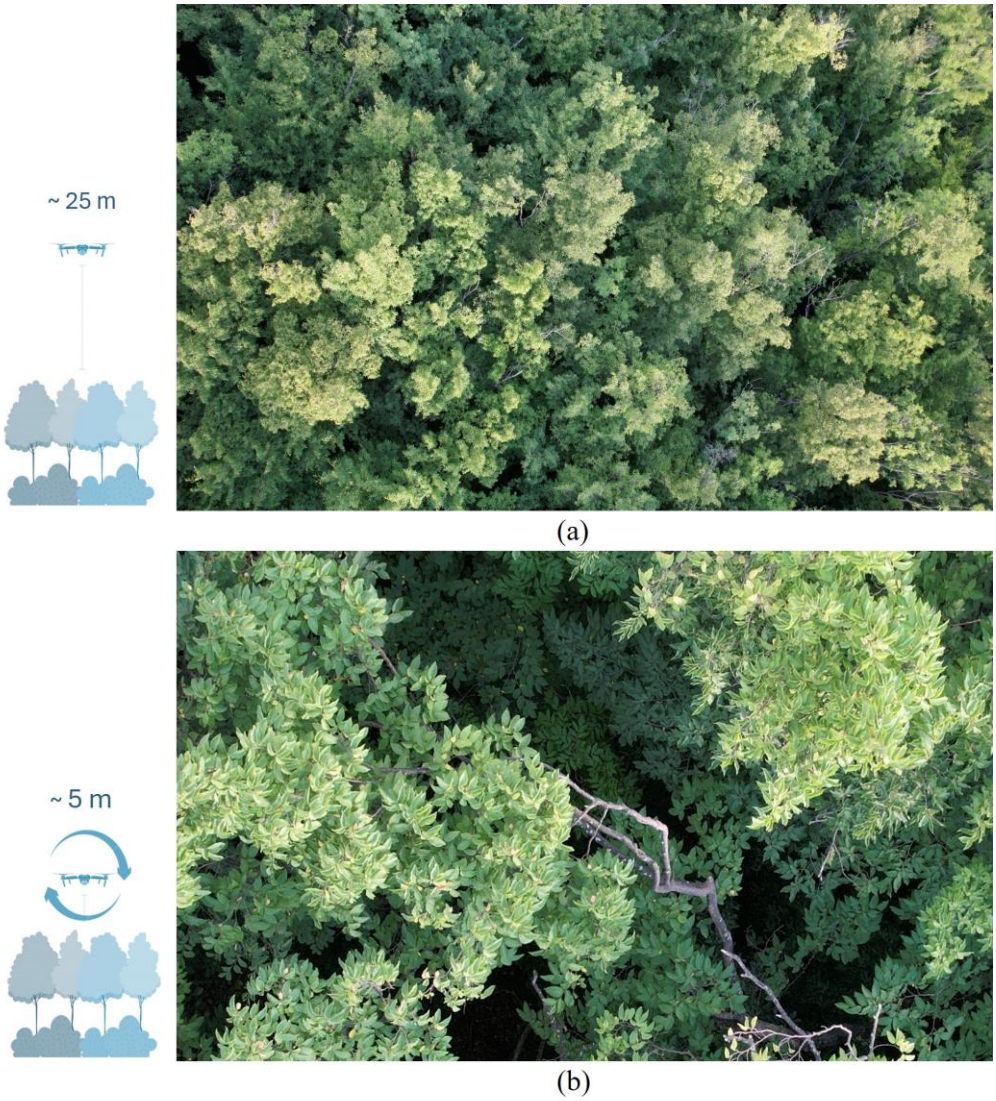

Figure 3. Drone photo acquisition at each survey point. Initially, an overhead photo (**a**) is captured from high above the canopy. This is followed by a close-range shot (**b**), providing a detailed view. Here, *Ostrya carpinifolia* is prominently visible. At this lower altitude, photos are taken in the four cardinal directions (north, east, south, and west) for species abundance estimation. Both photos were captured on 6 July 2022.

Table 1. Reference data. Target classes for the supervised map are listed. For physiognomic types, we report the dominant plant species and the corresponding habitat code (Annex 1 of the European Union Habitats Directive). The * denotes a priority habitat. In the case of 6210, it is an important orchid site (*). The habitats listed in square brackets are included in a mosaic pattern and/or are sporadically present within the reference category.

Label	Vegetation Types	Habitat Code	Plots
	Woodland		
O	Black hornbeam wood	-	278
Q	Downy-oak wood	91AA *	150
R	*Pinus* sp. plantations	-	136
L	Holm-oak wood	9340	94
F	Beech wood	9210 *	34
SP	Black poplar riparian wood	92A0, [3270, 3280, 6430]	35
SAL	White willow riparian wood	92A0, [3270, 3280, 6430]	15
	Shrublands		
GI	*Spartium junceum* shrub	-	60
JO	*Juniperus oxycedrus* shrub	-	20
JC	*Juniperus communis* shrub	5130	16
AR	*Salix eleagnos* riparian shrub	[3270, 3280, 6430, 92A0]	26
	Grasslands		
B	*Bromus erectus* grassland	6210 *, [6110 *, 6220 *]	71
	Garrigues and chasmophytic vegetation		
GA	*Artemisia alba* and *Satureja montana* garrigues	[6110 *, 6220 *]	57
PA	Vegetation of rocky slopes	[8210, 9340]	25
	Other		
CO	Crop land and post-crop vegetation	-	77
AV	Riverbed	[3270, 3280]	24
TOT			1118

For easily interpretable categories such as cropland, coniferous plantations and urban areas, which do not require field verifications or the use of high-resolution drone imagery, the target mapping classes were determined using high-resolution satellite images available on Google Earth [47]. The reference data are detailed in Table 1, while their spatial distribution is depicted in Figure 2b.

2.3. Vegetation Mapping by Supervised Functional Classification of Remote Sensing Time Series

2.3.1. Sentinel-2 Time Series and Functional Data Analysis (FDA)

We utilized 234 Sentinel-2 images for the period of 2019–2021 to generate multivariate (multispectral) weekly pixel-based time series for the entire study area, encompassing roughly 560,000 pixels. From all the available Sentinel-2 images, only the pixels affected by clouds, cloud shadows and snow were excluded, while the remaining clear observations were filtered to remove outliers and to estimate mean weekly smoothed and gap-filled time series using Generalized Additive Models (GAM) [48], as described by Balestra et al. [49] and Pesaresi et al. [50]. GAMs are advantageous as they do not require measurements to be uniformly distributed, which is beneficial since clouds and other data issues can cause random gaps in the data [51]. The GAM-smoothed and gap-filled time series were applied to the Sentinel-2 bands B2, B3, B4, B5, B6, B7, B8*, B11 and B12 (details on the Sentinel-2 bands can be found from the European Space Agency) [52]. Through this process, the original discrete time series of Sentinel-2 imagery were transformed into

regular weekly multispectral functions, representing seasonal variations for each pixel. These data were analyzed using a Multivariate Functional Principal Component Analysis (MFPCA), a technique that effectively captures joint variations among the functions. An MFPCA decomposes the data into a set of orthogonal multivariate functional principal components, or modes of functional variation (multivariate eigenfunctions), each associated with the corresponding eigenvalues and Multivariate Functional Principal Component (MFPC) scores. Unlike traditional multivariate methods, such as PCA, which treat data as independent observations, MFPCA leverages the fundamental philosophy of FDA by treating time series as single entities, explicitly preserving their temporal structure [53–55].

2.3.2. Topographic Features

Topographic features play a significant role in shaping vegetation distributions. Studies like that by Marcinkowska-Ochtyra et al. [56] has shown that incorporating these features alongside seasonal spectral variations can enhance the accuracy of supervised vegetation mapping. To this end, several topographic features were derived from the Digital Elevation Model (DEM) "TINITALY" [57], including altitude (m a.s.l.), slope (°), the Topographic Wetness Index (TWI), the Topographic Position Index (TPI) and the Diurnal Anisotropic Heat (DAH). To reduce redundancy and improve interpretability, these features were processed using a classical Principal Component Analysis (PCA).

2.3.3. Supervised Classification and Accuracy Evaluation

The Random Forest (RF) classifier, widely used in habitat mapping studies involving remote sensing data [58], was employed for the supervised vegetation mapping. Spectral seasonal variations (MFPC scores) and topographic characteristics (PCA scores) served as input predictors, with Recursive Feature Elimination applied to retain only the most significant features. To address the common issue of class imbalance in training and validation datasets, which can bias results and lead to the over-prediction of majority classes [18,59] the RF classifier was configured to use down-sampling. The model accuracy was assessed using overall accuracy (OA), producer accuracy (PA) and user accuracy (UA) metrics [60,61]. To ensure robust estimates and minimize bias, we implemented a 10-fold cross-validation repeated five times, resulting in a cross-validated confusion matrix.

For the supervised vegetation mapping workflow, several R packages were utilized as follows: *sen2r* (version 1.6.0) [62] for downloading Sentinel-2 images, *raster* (version 3.3-13) [63] for image processing, *forecast* (version 8.12) [64,65] and *mgcv* (version 1.8-33) [48] for constructing smoothed functions and *MFPCA* (version 1.3-6) [53] for decomposing and reducing the multivariate functional space. The Random Forest (RF) models and accuracy assessments were carried out using the R package *caret* version 6.0.86 [66].

3. Results

Figure 4a shows the weekly smoothed functions of seasonal variations across the spectral bands for each pixel in the study area. Using these functions, the MFPCA extracted the main components (MFPC components), or the principal orthogonal modes, of temporal variation throughout the year (Figure 4b). The proportion of variance explained by the identified functional components (eigenvalues) is reported in Figure A1. Figure 4b illustrates the temporal patterns of the first three MFPC components, which, together, account for 85.51% of the total variation.

The first component (MFPC1), which accounts for 48.55% of the total variation, distinguishes pixels with below-average reflectance values in bands B3, B4, B5, B11 and B12 throughout the year from those with above-average reflectance values. The second component (MFPC2), explaining 26.78% of the total variation, contrasts pixels with below-average

reflectance values in bands B6, B7 and B8 during the spring and summer months with those exhibiting significantly above-average reflectance values. The third component (MFPC3), accounting for 10.16% of the total variation, captures a pattern primarily occurring in winter for bands B6, B7 and B8, and during spring, summer and autumn for the other bands.

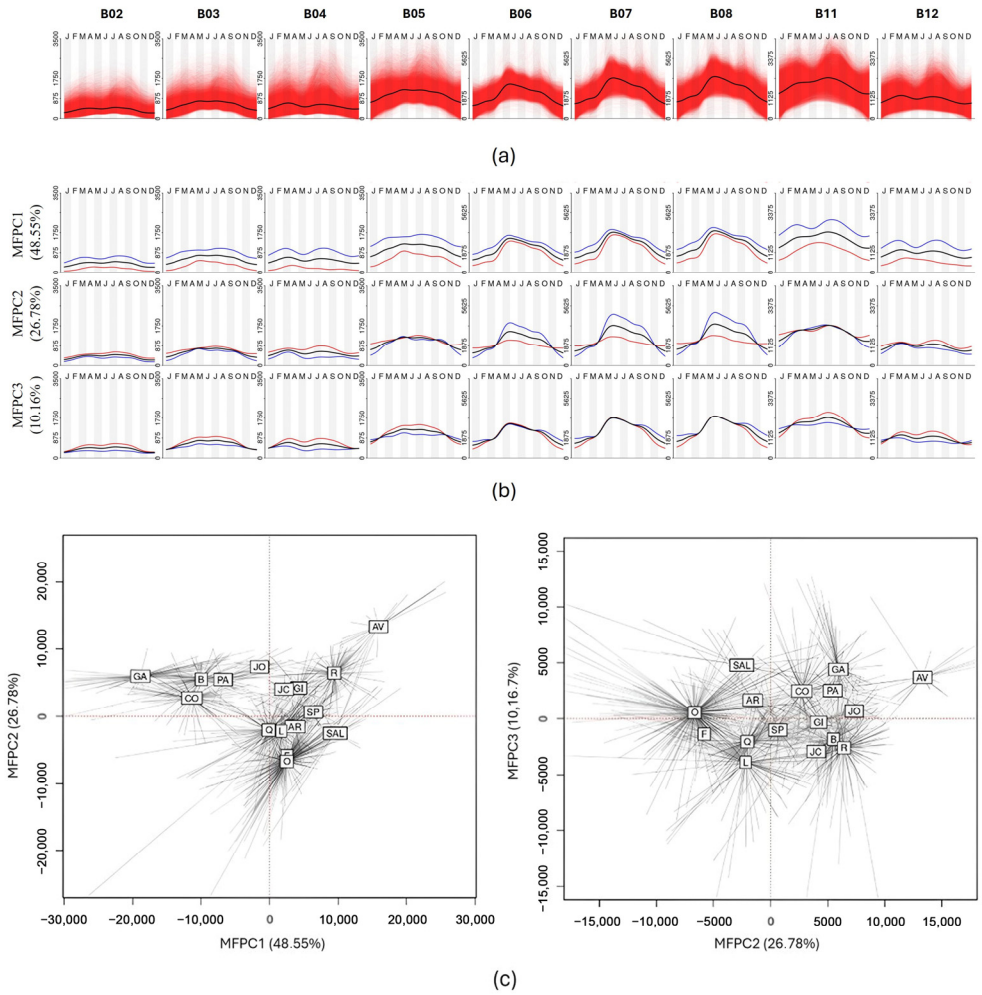

Figure 4. Graphical representation of the main findings from the Functional Data Analysis applied to the multispectral weekly time series of the Furlo area. (**a**) Seasonal profiles for all of the pixels in the study area, with the columns representing the nine Sentinel-2 bands analyzed. (**b**) The first three MFPCA components. The influence of these components on the overall means of the nine selected time series (depicted by the black line) is shown by adding (red line) or subtracting (blue line) a multiple (e.g., the median of the scores) of each principal functional component. (**c**) MFPCA ordination space based on the top three MFPCA components, enabling comparisons between vegetation types. The spider diagram illustrates the relationship between MFPC components and vegetation types, with the labels corresponding to Table 1.

Figure 4c illustrates the reduced MFPCA ordination (phenological) space defined by the scores of the first three MFPC components. The overlay of target classes, represented as spider plots, reveals that each class occupies a distinct sector of the ordination space, indicating clear differences in their seasonal behaviors throughout the year. These behaviors are related to variations across the spectral bands and are further detailed by the mean multispectral seasonal profiles shown in Figure 5.

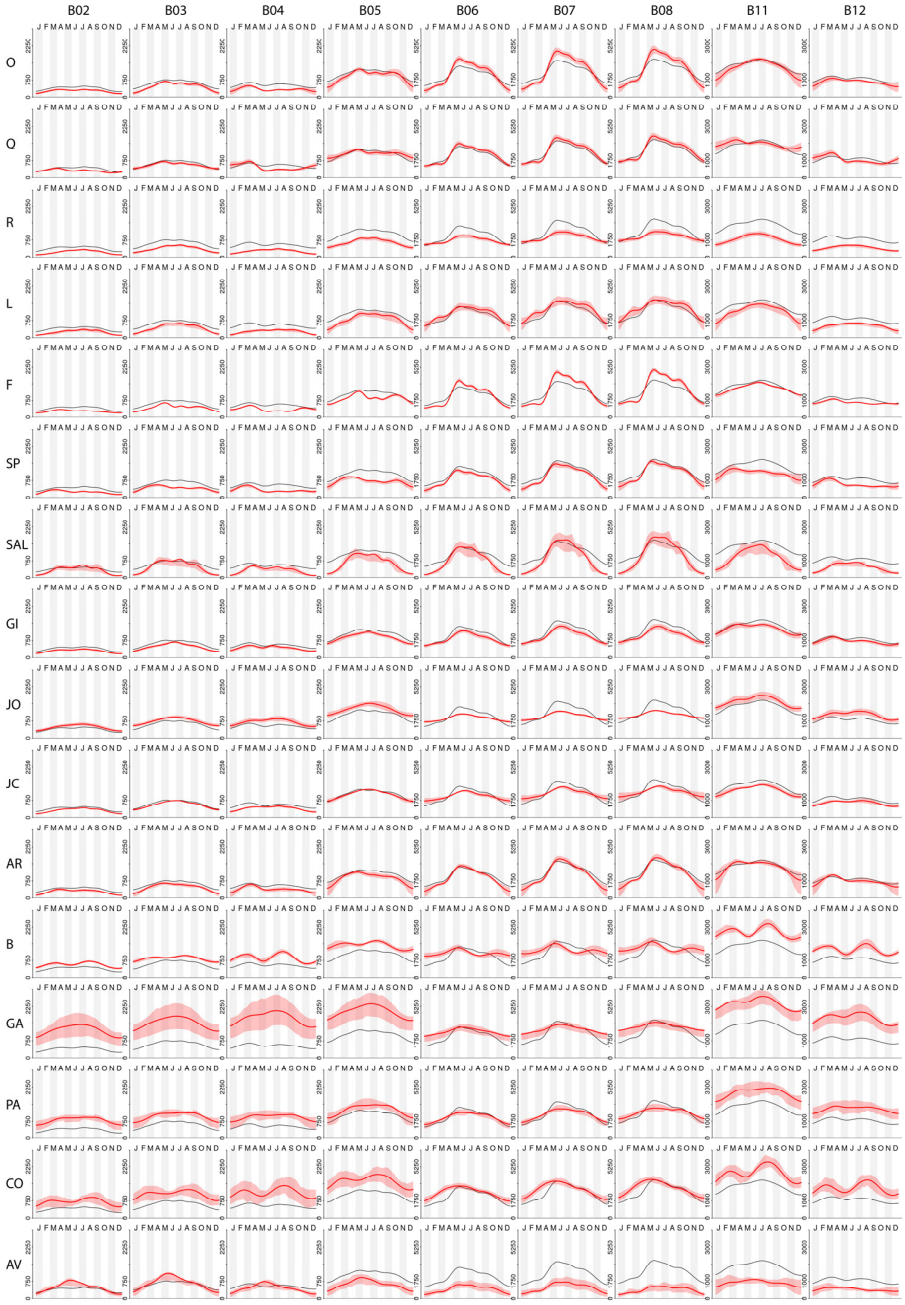

Figure 5. Seasonal temporal profiles of the target classes across various spectral bands correspond to the 1118 reference data points. The bold red line represents the mean vegetation band variation. The red polygon shows the 10th–90th percentile range. The black line represents the mean vegetation band variation for the entire study area. The row acronyms denote the plant associations and habitats listed in Table 1, while the columns refer to the different Sentinel-2 bands.

The supervised Random Forest (RF) classification of seasonal spectral variations (MFPC scores), combined with the topographic characteristics (PC scores), achieved an OA of 92.59% and the vegetation map obtained is presented in Figure 6. The confusion matrix (Table 2) indicates that the PA ranges from 73.3% to 97.3%, while the UA varies between 83.3% and 100%. The five most important predictors for the Random Forest model, ranked by the Mean Decrease Accuracy index, are as follows: MFPC2 (100.00%), MFPC1 (67.07%), MFPC4 (65.84%), MFPC7 (37.86%) and MFPC3 (23.96%). These predictors were extracted through an MFPCA from weekly smoothed multispectral seasonal variations. When Random Forest was applied exclusively to the seasonal spectral variations, it achieved an

OA of 91.19%. Conversely, applying the Random Forest solely to topographic features resulted in an OA of 61.63%.

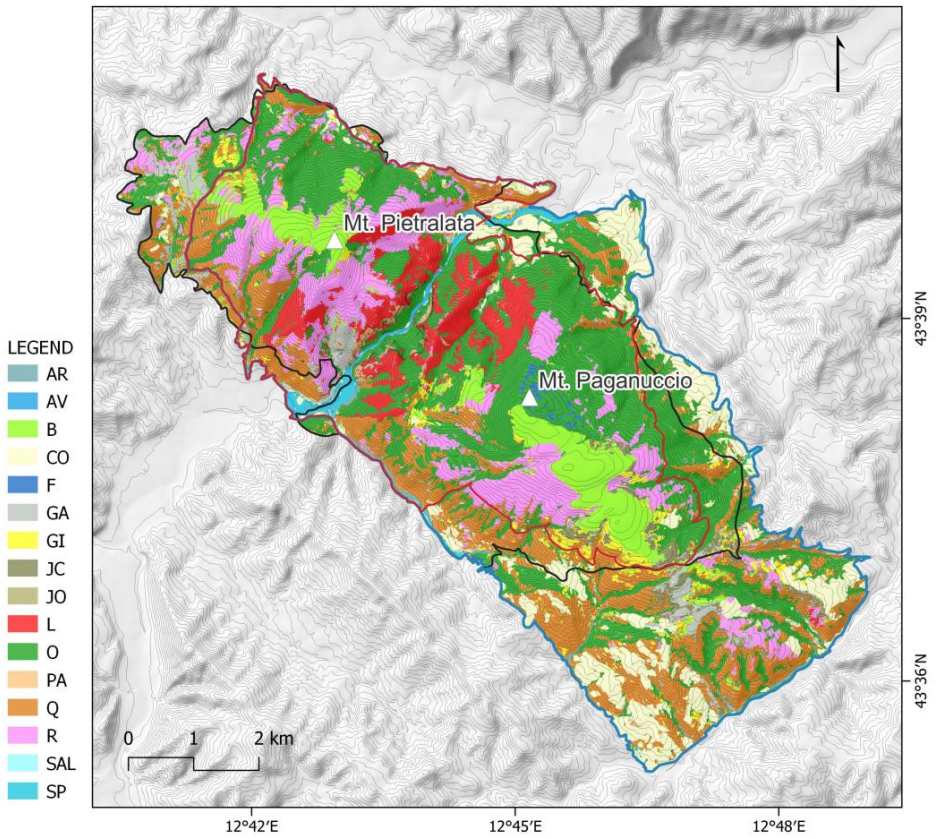

Figure 6. Vegetation and habitats map of study area: the map was obtained by the supervised random forest classification of the main seasonal remotely sensed phenological variations, as well as the main topographic predictors. The legend acronyms correspond to the plant associations and habitats listed in Table 1. The boundaries of the Gola del Furlo State Nature Reserve are outlined in black, that of the Special Protection Area (SPA) "Furlo" (code: IT5310029) are outlined in blue, and that of the Special Area of Conservation (SAC) "Gola del Furlo" (IT5310016) are outlined in red.

Table 2. Cross-validated confusion matrix (10-fold, repeated five times) between the predicted target classes of the study area. The overall accuracy (OA), producer accuracy (PA), user accuracy (UA), and K statistic are given. The row and column acronyms denote the plant associations and habitats listed in Table 1.

		Reference Data																
		AR	**AV**	**B**	**CO**	**F**	**GA**	**GI**	**JC**	**JO**	**L**	**O**	**PA**	**Q**	**R**	**SAL**	**SP**	**UA**
Prediction	**AR**	2.2	0.0	0.0	0.0	0.0	0.0	0.0	0.0	0.0	0.0	0.0	0.0	0.0	0.0	0.0	0.1	94.0
	AV	0.0	2.0	0.0	0.0	0.0	0.0	0.0	0.0	0.0	0.0	0.0	0.0	0.0	0.0	0.0	0.0	100.0
	B	0.0	0.0	5.8	0.2	0.0	0.4	0.1	0.0	0.0	0.0	0.0	0.0	0.1	0.0	0.0	0.0	88.8
	CO	0.0	0.0	0.1	6.2	0.0	0.0	0.0	0.0	0.0	0.0	0.0	0.0	0.0	0.0	0.0	0.0	98.3
	F	0.0	0.0	0.0	0.0	2.9	0.0	0.0	0.0	0.0	0.0	0.0	0.0	0.0	0.0	0.0	0.0	100.0
	GA	0.0	0.0	0.3	0.2	0.0	4.5	0.0	0.0	0.0	0.0	0.0	0.1	0.0	0.0	0.0	0.0	89.3
	GI	0.0	0.0	0.1	0.0	0.0	0.0	4.8	0.2	0.0	0.0	0.0	0.0	0.0	0.2	0.0	0.0	91.5
	JC	0.0	0.0	0.0	0.0	0.0	0.0	0.0	1.1	0.0	0.0	0.0	0.0	0.0	0.0	0.0	0.0	100.0
	JO	0.0	0.0	0.0	0.0	0.0	0.1	0.0	0.0	1.5	0.0	0.0	0.0	0.0	0.2	0.0	0.0	83.3
	L	0.0	0.0	0.0	0.0	0.0	0.0	0.0	0.0	0.0	7.9	0.1	0.1	0.0	0.2	0.0	0.0	95.6
	O	0.1	0.0	0.0	0.2	0.2	0.0	0.1	0.0	0.0	0.4	24.2	0.0	1.3	0.1	0.1	0.1	90.4
	PA	0.0	0.0	0.0	0.0	0.0	0.0	0.0	0.0	0.0	0.0	0.0	2.1	0.0	0.0	0.0	0.0	98.3
	Q	0.0	0.0	0.0	0.1	0.0	0.1	0.1	0.0	0.3	0.0	0.5	0.0	12.0	0.0	0.0	0.0	91.8
	R	0.0	0.0	0.1	0.0	0.0	0.0	0.3	0.2	0.0	0.2	0.0	0.0	0.0	11.6	0.1	0.0	93.5
	SAL	0.0	0.0	0.0	0.0	0.0	0.0	0.0	0.0	0.0	0.0	0.1	0.0	0.0	0.0	1.0	0.0	91.7
	SP	0.0	0.1	0.0	0.0	0.0	0.0	0.0	0.0	0.0	0.0	0.0	0.0	0.0	0.0	0.1	2.9	93.1
	PA	96.2	93.3	91.3	90.4	94.1	87.7	89.3	75.0	85.0	93.4	97.3	93.6	89.5	95.1	73.3	92.6	

Table 2. *Cont.*

	Reference Data																
	AR	**AV**	**B**	**CO**	**F**	**GA**	**GI**	**JC**	**JO**	**L**	**O**	**PA**	**Q**	**R**	**SAL**	**SP**	**UA**
OA	92.59 (±2.21)																
K	0.91 (±0.02)																

4. Discussion

4.1. Main Results

The integration of drone truthing with the supervised classification of seasonal spectral variations enabled the production of a highly accurate vegetation and habitat map, achieving an OA of 92.59%. This significantly exceeds the 80% threshold, a benchmark rarely reached in remote sensing for habitat mapping [67]. This result is particularly noteworthy given the large number of target classes (16 in the study area), especially considering that accuracy often decreases as the number of mapping categories increases [9,68–70]. The effectiveness and efficiency of this methodology offer promising opportunities for detailed and reliable vegetation and habitat mapping. It allows for regular updates and the repetition of mapping efforts, even in large or complex areas, resulting in significant time and cost savings. This makes it a valuable tool for monitoring vegetation dynamics and assessing the conservation status of habitats [8].

The drone truthing activities allowed for the following: (i) the acquisition of high-resolution images, which are useful for botanists to identify dominant plant species and assign each survey area to one of the mapping categories listed in Table 1; and (ii) the strict adherence to a plot-based sampling design (Figure 2b). These two features facilitated the creation of a dense and spatially balanced reference dataset that is highly representative of the spectral variability of vegetation, including areas that are difficult to access (Figure 7), all within a short timeframe. This would be difficult to achieve with traditional methods [9,71–73].

Figure 7. Forested area, photographed on 7 October 2022, which was challenging to survey with traditional methods due to its inaccessibility and complex topography, which would have required considerable time.

The high map accuracy achieved demonstrates that the high quality of the reference data significantly contributed to the optimal training of the classifier. It also highlights the substantial informational value of seasonal multispectral remote sensing variations, linked to the different phenological stages of vegetation, in ensuring accurate mapping [14–17,74]. The Random Forest identified both the seasonal variations with a higher explained variance (MFPC1, MFPC2) and those with a lower variance (e.g., MFPC7, MFPC4) as important.

Seasonal spectral variations contributed significantly more to the OA than topographic features, aligning with the findings by Zhu and Liu [75], Barrett et al. [76], Marcinkowska-Ochtyra et al. [56] and Rapinel et al. [15]. However, topographic predictors proved crucial for certain classes, such as riparian woodlands, located in complex terrains like the Furlo Gorge. In these areas, spectral variations can be distorted, making topographic data essential for achieving accurate classification.

4.2. Benefits for Habitat Directive, Phytosociology, and Landscape Management

The use of the reference data obtained through drone truthing resulted in a higher OA (92.59%) compared to similar studies using the same classification methodology but relying solely on the reference data collected through traditional ground truthing. A key achievement is the successful classification of specific categories of notable interest within Annex I of the Habitats Directive, such as the downy oak woodland, a priority habitat (91AA*), with a PA of 89.5% and a UA of 91.8%, distinguishing it from the hornbeam woodland (PA 97.3% and UA 90.4%). These categories, previously misclassified [18,19,50], showed improvement thanks to a denser and more balanced reference dataset, collected using drone truthing rather than traditional ground truthing methods.

The ability to produce accurate, up-to-date, and repeatable vegetation and habitat maps with significant time and cost savings opens new avenues for landscape monitoring and habitat management [77,78]. This approach aligns with the requirements of European environmental policies, such as the Habitats Directive, which mandate updates every six years [3]. By enabling continuous habitat monitoring, this approach facilitates diachronic analyses of data collected through consistent methodologies, making it possible to evaluate the long-term impacts of conservation policies and implement targeted, adaptive interventions. From this perspective, the methodology could prove particularly valuable within the framework of the Nature Restoration Law [79], which aims to restore at least 20% of the degraded habitats by 2030, both in identifying areas that are more sensitive to change and in monitoring and evaluating the effectiveness of interventions (e.g., shrub and grass encroachment in grasslands of habitat 6210) [80–83]. For this purpose, drone-based imagery serves as an invaluable tool for documenting the environmental changes over time, creating a high-resolution photographic archive [41] of vegetation categories to support precise habitat assessments and restoration efforts.

In addition, it should be highlighted that the Sentinel-2 time series, expressed as weekly multispectral seasonal smoothed functions and analyzed with MFPCA, offer a compact and parsimonious model with graphically interpretable results. This approach enhances the understanding of key seasonal variations and phenological behaviors across vegetation types and habitats (e.g., Figures 4 and 5).

These insights assist botanists and ecologists in analyzing the relationships between field observations and remotely sensed data. Additionally, they complement species-based approaches in plant community ecology and phytosociology, such as the Braun-Blanquet method [82–85].

4.3. Limits and Future Works

Despite the significant advantages offered by drone-based truthing activities in this study, some limitations were encountered that, if addressed, could make the processes

even more efficient and accurate. One limitation was related to the drone's specifications. For example, the lack of a precise distance estimation system and optical zoom capability required close flyovers for detailed species identification. While high-resolution images were obtained, the ground sample distance (GSD) likely varied because a constant vertical distance from the canopy could not be ensured. This resulted in the absence of a fully standardized procedure [86]. However, these limitations can be addressed by using drones with more advanced equipment [41], enabling a precise and standardized protocol that would enhance data collection efficiency, safety and the reliability of analysis, improving result robustness and comparability. Another limitation encountered during drone operations was the difficulty of maintaining a Visual Line of Sight (VLOS) in areas with complex terrain morphology, which can obstruct visual contact and disrupt the drone's radio signal. These obstacles necessitated frequent changes in the take-off point, resulting in significant time delays and increased battery consumption. To address this, pre-survey visibility analyses using a digital terrain model would help to identify optimal take-off locations, allowing for the coverage of the maximum number of points with a single launch, thereby ensuring safer and more efficient operations.

5. Conclusions

In conclusion, the results of this study demonstrate that our approach improves the efficiency of supervised phytosociological mapping by addressing a critical challenge in the field: the collection of high-quality reference data [9,36]. While traditional ground-based verification methods (e.g., the Braun-Blanquet approach) require significant efforts and are often unfeasible, this approach helps to bridge the gap between intensive field surveys and remotely sensed data [87], making it valuable for supervised vegetation mapping using remotely sensed time series.

The ability to generate reproducible, updatable and comparable maps opens new opportunities for continuous vegetation and habitat monitoring, offering valuable tools for predicting and managing changes. This can provide critical information to managing authorities and improve landscape conservation practices [8].

Traditional phytosociological knowledge, which is collected with significant effort in the field, remains a fundamental aspect of vegetation mapping, especially when it is effectively spatialized and updated over time. For this reason, we consider drone-based ground-truthing activities not as a replacement for traditional methods, such as the Braun-Blanquet approach, but as a complementary tool. Much like a botanist uses a hand lens to examine diagnostic features or a spade to collect a specimen, drones provide an additional means to enhance fieldwork. They enable botanists and phytosociologists to efficiently identify diagnostic species and assign plots to vegetation types that would otherwise be difficult or impossible to access, especially in complex landscapes like the one studied here, where traditional methods alone would be insufficient [38,40,41,88].

Finally, to further enhance the efficiency of this method, future studies could explore the integration of AI, deep learning and machine learning techniques for automated species recognition and abundance estimation [89–93]. These advancements could optimize the creation of reference data, particularly by expediting the assignment of plots to target mapping categories, thereby improving the overall speed and accuracy of the mapping process.

Author Contributions: Conceptualization, S.P. and G.Q.; reference data collection and management, S.P., G.Q., S.C. and N.H.; data analysis and programming, S.P., A.M. and G.Q.; methodology, S.P., A.M., S.C. and G.Q.; writing—original draft preparation, S.P., G.Q. and N.H.; writing—review and editing, S.P., G.Q., N.H. and S.C.; supervision, S.P., A.M. and S.C. All authors have read and agreed to the published version of the manuscript.

Funding: This research received no external funding.

Data Availability Statement: The original contributions presented in this study are included in the article. Further inquiries can be directed to the corresponding author.

Acknowledgments: Our acknowledgments are extended to the Province of Pesaro and Urbino for granting the authorization for drone flights (protocol no. 27125/2021) within the Gola del Furlo State Nature Reserve and for their support in the habitat mapping project.

Conflicts of Interest: The authors declare no conflicts of interest.

Appendix A

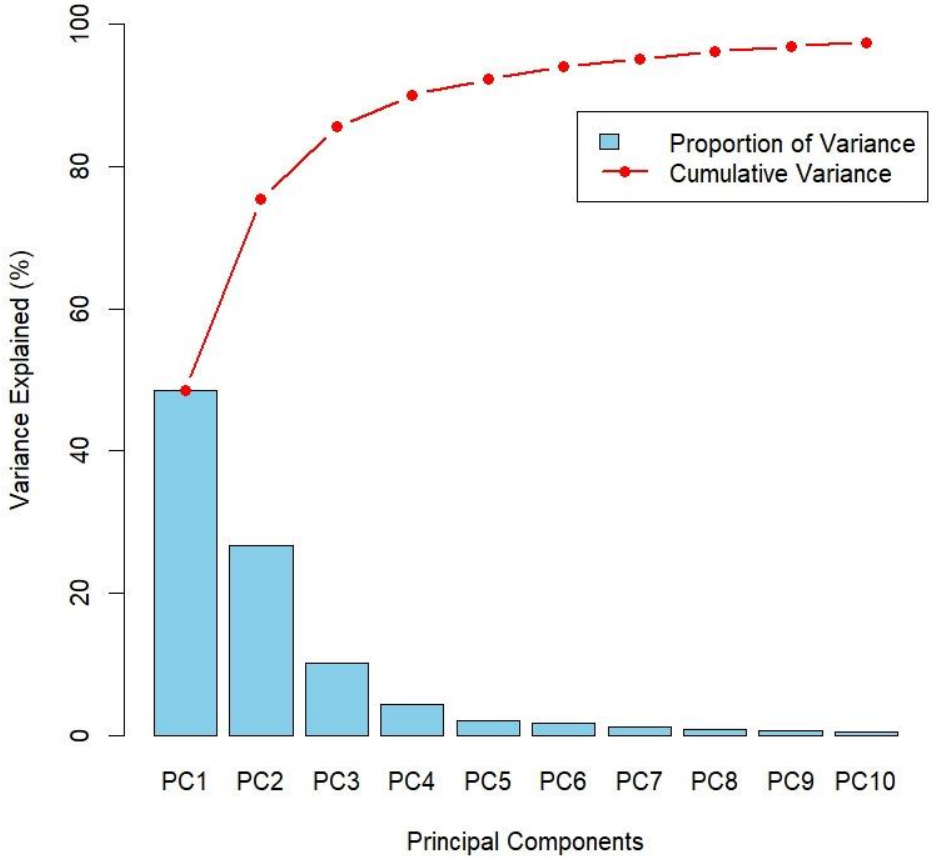

Figure A1. Proportion of variance explained by the identified functional components (eigenvalues). The bar plot shows the proportion of variance explained by each principal component, with the cumulative variance illustrated by the red line. The first three components individually explain 48.55%, 26.79%, and 10.17% of the variance, respectively, accounting for a combined total of 85.51% of the variance. Collectively, the first 10 components account for 97.40% of the total variance.

Table A1. Target classes of the reference data with corresponding plant associations (syntaxa name). In most cases, each physiognomic vegetation type corresponds to a single plant association (e.g., beech wood), while some, such as holm oak and black hornbeam forests, encompass multiple associations.

Label	Vegetation Types	Plant Associations
	Woodland	
O	Black hornbeam wood	*Scutellario columnae-Ostryetum carpinifoliae*; *Asparago acutifoliii-Ostryetum carpinifoliae*; *Anemono trifoliae-Ostryetum carpinifoliae*
Q	Downy-oak wood	*Roso sempervirentis-Quercetum pubescentis*; *Cytiso sessilifolii-Quercetum pubescentis*
R	*Pinus* sp. plantations	Coniferous plantings (*Pinus* ssp., *Cupressus* ssp., *Hesperocyparis* ssp.)

Table A1. *Cont.*

Label	Vegetation Types	Plant Associations
L	Holm-oak wood	*Cyclamino hederifolii-Quercetum ilicis*; *Cephalanthero longifoliae-Quercetum ilicis*
F	Beech wood	*Lathyro veneti-Fagetum sylvaticae*
SP	Black poplar riparian wood	*Salici albae-Populetum nigrae*
SAL	White willow riparian wood	*Rubo ulmifolii-Salicetum albae*
	Shrublands	
GI	*Spartium junceum* shrub	*Spartio juncei-Cytisetum sessilifolii* var. a *Spartium junceum*
JO	*Juniperus oxycedrus* shrub	*Spartio juncei-Cytisetum sessilifolii* var. a *Juniperus oxycedrus*
JC	*Juniperus communis* shrub	*Juniperetum oxycedri-communis*
AR	*Salix eleagnos* riparian shrub	*Salicetum elaeagni*
	Grasslands	
B	*Bromus erectus* grassland	*Brizo mediae-Brometum erecti*; *Asperulo purpureae-Brometum erecti*; *Helianthemo apenninae-Festucetum circummediterraneae*;
	Garrigues and chasmophytic vegetation	
GA	*Artemisia alba* and *Satureja montana* garrigues	*Potentillo arenariae-Artemisietum albae*; *Cephalario leucanthae-Saturejetum montanae*
PA	Vegetation of rocky slopes	*Moehringio papulosae-Potentilletum caulescentis*; *Saxifrago australis-Trisetetum bertolonii*
	Other	
CO	Crop land and post-crop vegetation	Agricultural crops (sowings, alfalfa and production tree plantations) and post-harvest crops
AV	Riverbed	

References

1. Chytrý, M.; Schaminée, J.H.J.; Schwabe, A. Vegetation Survey: A New Focus for Applied Vegetation Science. *Appl. Veg. Sci.* **2011**, *14*, 435–439. [CrossRef]
2. Mucina, L. Europe, Ecosystems of. In *Encyclopedia of Biodiversity*, 2nd ed.; Elsevier Inc.: Amsterdam, The Netherlands, 2013; pp. 333–346, ISBN 9780123847195.
3. CEC. Council Directive 92/43/EEC of 21 May 1992 on the Conservation of Natural Habitats and of Wild Fauna and Flora. *Off. J. Eur. Union* **1992**, *206*, 7–50.
4. Rodwell, J.S.; Evans, D.; Schaminée, J.H.J. Phytosociological Relationships in European Union Policy-Related Habitat Classifications. *Rend. Lincei Sci. Fis. Nat.* **2018**, *29*, 237–249. [CrossRef]
5. Biondi, E. Phytosociology Today: Methodological and Conceptual Evolution. *Plant Biosyst.* **2011**, *145*, 19–29. [CrossRef]
6. Biondi, E.; Burrascano, S.; Casavecchia, S.; Copiz, R.; Del Vico, E.; Galdenzi, D.; Gigante, D.; Lasen, C.; Spampinato, G.; Venanzoni, R.; et al. Diagnosis and Syntaxonomic Interpretation of Annex I Habitats (Dir. 92/43/EEC) in Italy at the Alliance Level. *Plant Sociol.* **2012**, *49*, 5–37. [CrossRef]
7. Evans, D. The Habitats of the European Union Habitats Directive. *Biol. Environ. Proc. R. Ir. Acad.* **2006**, *106B*, 167–173. [CrossRef]
8. Ichter, J.; Savio, L.; Evans, D.; Poncet, L. State-of-the-Art of Vegetation Mapping in Europe: Results of a European Survey and Contribution to the French Program CarHAB. *Doc. Phytosociol. Série 3* **2017**, *6*, 335–352.
9. Rapinel, S.; Rozo, C.; Delbosc, P.; Bioret, F.; Bouzillé, J.B.; Hubert-Moy, L. Contribution of Free Satellite Time-Series Images to Mapping Plant Communities in the Mediterranean Natura 2000 Site: The Example of Biguglia Pond in Corse (France). *Mediterr. Bot.* **2020**, *41*, 181–191. [CrossRef]
10. Gigante, D.; Attorre, F.; Venanzoni, R.; Acosta, A.T.R.; Agrillo, E.; Aleffi, M.; Alessi, N.; Allegrezza, M.; Angelini, P.; Angiolini, C.; et al. A Methodological Protocol for Annex i Habitats Monitoring: The Contribution of Vegetation Science. *Plant Sociol.* **2016**, *53*, 77–87. [CrossRef]
11. Tarantino, C.; Forte, L.; Blonda, P.; Vicario, S.; Tomaselli, V.; Beierkuhnlein, C.; Adamo, M. Intra-Annual Sentinel-2 Time-Series Supporting Grassland Habitat Discrimination. *Remote Sens.* **2021**, *13*, 277. [CrossRef]
12. Hubert-Moy, L.; Fabre, E.; Rapinel, S. Contribution of SPOT-7 Multi-Temporal Imagery for Mapping Wetland Vegetation. *Eur. J. Remote Sens.* **2020**, *53*, 201–210. [CrossRef]
13. Feret, J.B.; Corbane, C.; Alleaume, S. Detecting the Phenology and Discriminating Mediterranean Natural Habitats with Multispectral Sensors-An Analysis Based on Multiseasonal Field Spectra. *IEEE J. Sel. Top. Appl. Earth Obs. Remote Sens.* **2015**, *8*, 2294–2305. [CrossRef]

14. Marzialetti, F.; Giulio, S.; Malavasi, M.; Sperandii, M.G.; Acosta, A.T.R.; Carranza, M.L. Capturing Coastal Dune Natural Vegetation Types Using a Phenology-Based Mapping Approach: The Potential of Sentinel-2. *Remote Sens.* **2019**, *11*, 1506. [CrossRef]
15. Rapinel, S.; Mony, C.; Lecoq, L.; Clément, B.; Thomas, A.; Hubert-Moy, L. Evaluation of Sentinel-2 Time-Series for Mapping Floodplain Grassland Plant Communities. *Remote Sens. Environ.* **2019**, *223*, 115–129. [CrossRef]
16. Stendardi, L.; Karlsen, S.R.; Niedrist, G.; Gerdol, R.; Zebisch, M.; Rossi, M.; Notarnicola, C. Exploiting Time Series of Sentinel-1 and Sentinel-2 Imagery to Detect Meadow Phenology in Mountain Regions. *Remote Sens.* **2019**, *11*, 542. [CrossRef]
17. Vrieling, A.; Meroni, M.; Darvishzadeh, R.; Skidmore, A.K.; Wang, T.; Zurita-Milla, R.; Oosterbeek, K.; O'Connor, B.; Paganini, M. Vegetation Phenology from Sentinel-2 and Field Cameras for a Dutch Barrier Island. *Remote Sens. Environ.* **2018**, *215*, 517–529. [CrossRef]
18. Pesaresi, S.; Mancini, A.; Quattrini, G.; Casavecchia, S. Functional Analysis for Habitat Mapping in a Special Area of Conservation Using Sentinel-2 Time-Series Data. *Remote Sens.* **2022**, *14*, 1179. [CrossRef]
19. Pesaresi, S.; Mancini, A.; Quattrini, G.; Casavecchia, S. Mapping Mediterranean Forest Plant Associations and Habitats with Functional Principal Component Analysis Using Landsat 8 NDVI Time Series. *Remote Sens.* **2020**, *12*, 1132. [CrossRef]
20. Čahojová, L.; Ambroz, M.; Jarolímek, I.; Kollár, M.; Mikula, K.; Šibík, J.; Šibíková, M. Exploring Natura 2000 Habitats by Satellite Image Segmentation Combined with Phytosociological Data: A Case Study from the Čierny Balog Area (Central Slovakia). *Sci. Rep.* **2022**, *12*, 18375. [CrossRef]
21. Pasquarella, V.J.; Holden, C.E.; Woodcock, C.E. Improved Mapping of Forest Type Using Spectral-Temporal Landsat Features. *Remote Sens. Environ.* **2018**, *210*, 193–207. [CrossRef]
22. Schmidt, T.; Schuster, C.; Kleinschmit, B.; Förster, M. Evaluating an Intra-Annual Time Series for Grassland Classification—How Many Acquisitions and What Seasonal Origin Are Optimal? *IEEE J. Sel. Top. Appl. Earth Obs. Remote Sens.* **2014**, *7*, 3428–3439. [CrossRef]
23. Ivanova, N. Global Overview of the Application of the Braun-Blanquet Approach in Research. *Forests* **2024**, *15*, 937. [CrossRef]
24. Yeo, S.; Lafon, V.; Alard, D.; Curti, C.; Dehouck, A.; Benot, M.L. Classification and Mapping of Saltmarsh Vegetation Combining Multispectral Images with Field Data. *Estuar. Coast. Shelf Sci.* **2020**, *236*, 106643. [CrossRef]
25. Ichter, J.; Evans, D.; Richard, D. *Terrestrial Habitat Mapping in Europe: An Overview*; Poncet, L., Spyropoulou, R., Martins, I.P., Eds.; MNHN-EEA: Luxembourg, 2014; Volume 1, ISBN 978-92-9213-420-4.
26. Waldner, F.; Hansen, M.C.; Potapov, P.V.; Löw, F.; Newby, T.; Ferreira, S.; Defourny, P. National-Scale Cropland Mapping Based on Spectral-Temporal Features and Outdated Land Cover Information. *PLoS ONE* **2017**, *12*, e0181911. [CrossRef] [PubMed]
27. Oldeland, J.; Dorigo, W.; Lieckfeld, L.; Lucieer, A.; Jürgens, N. Combining Vegetation Indices, Constrained Ordination and Fuzzy Classification for Mapping Semi-Natural Vegetation Units from Hyperspectral Imagery. *Remote Sens. Environ.* **2010**, *114*, 1155–1166. [CrossRef]
28. Chen, X.; Cao, X.; Chen, J.; Cui, X. Effect of Training Strategy on PUL-SVM Classification for Cropland Mapping by Landsat Imagery. In Proceedings of the 2015 IEEE International Geoscience and Remote Sensing Symposium (IGARSS), Milan, Italy, 26–31 July 2015; pp. 417–420.
29. Guo, Q.; Li, W.; Liu, D.; Chen, J. A Framework for Supervised Image Classification with Incomplete Training Samples. *Photogramm. Eng. Remote Sens.* **2012**, *78*, 595–604. [CrossRef]
30. Foody, G.M.; Pal, M.; Rocchini, D.; Garzon-Lopez, C.X.; Bastin, L. The Sensitivity of Mapping Methods to Reference Data Quality: Training Supervised Image Classifications with Imperfect Reference Data. *ISPRS Int. J. Geoinf.* **2016**, *5*, 199. [CrossRef]
31. Fu, Y.; Shen, R.; Song, C.; Dong, J.; Han, W.; Ye, T.; Yuan, W. Exploring the Effects of Training Samples on the Accuracy of Crop Mapping with Machine Learning Algorithm. *Sci. Remote Sens.* **2023**, *7*, 100081. [CrossRef]
32. Guo, Y.; Jia, X.; Paull, D.; Zhang, J.; Farooq, A.; Chen, X.; Islam, M.N. A Drone-Based Sensing System to Support Satellite Image Analysis for Rice Farm Mapping. In Proceedings of the IEEE International Geoscience & Remote Sensing Symposium, Yokohama, Japan, 2 August 2019; pp. 9376–9379.
33. Stehman, S.V.; Foody, G.M. Key Issues in Rigorous Accuracy Assessment of Land Cover Products. *Remote Sens. Environ.* **2019**, *231*, 111199. [CrossRef]
34. Tuia, D.; Persello, C.; Bruzzone, L. Domain Adaptation for the Classification of Remote Sensing Data: An Overview of Recent Advances. *IEEE Geosci. Remote Sens. Mag.* **2016**, *4*, 41–57. [CrossRef]
35. Banko, G. A Review of Assessing the Accuracy of Classifications of Remotely Sensed Data and of Methods Including Remote Sensing Data in Forest Inventory. 1998. Available online: https://www.researchgate.net/publication/23738314_A_Review_of_Assessing_the_Accuracy_of_Classifications_of_Remotely_Sensed_Data_and_of_Methods_Including_Remote_Sensing_Data_in_Forest_Inventory (accessed on 5 January 2025).
36. Vanden Borre, J.; Spanhove, T.; Haest, B. Towards a Mature Age of Remote Sensing for Natura 2000 Habitat Conservation: Poor Method Transferability as a Prime Obstacle. In *The Roles of Remote Sensing in Nature Conservation*; Díaz-Delgado, R., Lucas, R., Hurford, C., Eds.; Springer International Publishing: Cham, Switzerland, 2017; pp. 11–37. ISBN 978-3-319-64332-8.

37. Piel, A.K.; Crunchant, A.; Knot, I.E.; Chalmers, C.; Fergus, P.; Mulero-Pázmány, M.; Wich, S.A. Non Invasive Technologies for Primate Conservation in the 21st Century. *Int. J. Primatol.* **2022**, *43*, 133–167. [CrossRef]
38. Suir, G.M.; Saltus, C.L.; Sasser, C.E.; Harris, J.M.; Reif, M.K.; Diaz, R.; Giffin, G. *Evaluating Drone Truthing as an Alternative to Ground Truthing: An Example with Wetland Plant Identification*; ERDC/TN APCRP-MI-9; Engineer Research and Development Center: Vicksburg, MI, USA, 2021. [CrossRef]
39. Szantoi, Z.; Smith, S.E.; Strona, G.; Koh, L.P.; Wich, S.A. Mapping Orangutan Habitat and Agricultural Areas Using Landsat OLI Imagery Augmented with Unmanned Aircraft System Aerial Photography. *Int. J. Remote Sens.* **2017**, *38*, 2231–2245. [CrossRef]
40. Husson, E.; Hagner, O.; Ecke, F. Unmanned Aircraft Systems Help to Map Aquatic Vegetation. *Appl. Veg. Sci.* **2014**, *17*, 567–577. [CrossRef]
41. Nyberg, B.; Bairos, C.; Brimhall, M.; Deans, S.M.; Hanser, S.; Heintzman, S.; Hillmann Kitalong, A.; Menezes de Sequeira, M.; Nobert, N.; Rønsted, N.; et al. The Conservation Impact of Botanical Drones: Documenting and Collecting Rare Plants from Vertical Cliffs and Other Hard-to-Reach Areas. *Ecol. Solut. Evid.* **2024**, *5*, 12318. [CrossRef]
42. Jianya, G.; Haigang, S.; Guorui, M.; Qiming, Z. A Review of Multi-Temporal Remote Sensing Data Change Detection Algorithms. *Int. Arch. Photogramm. Remote Sens. Spat. Inf. Sci. ISPRS Arch.* **2008**, *37*, 757–762.
43. Rivas-Martínez, S.; Rivas Sáenz, S.; Penas, A.; Alcaraz, F.; Amigo, J.; Asensi, A.; Barbour, M.; Biondi, E.; Cantó, P.; Capelo, J.; et al. Worldwide Bioclimatic Classification System. *Glob. Geobot.* **2011**, *1*, 1–634.
44. Pesaresi, S.; Biondi, E.; Casavecchia, S. Bioclimates of Italy. *J. Maps* **2017**, *13*, 955–960. [CrossRef]
45. Braun-Blanquet, J.; Conard, H.S.; Fuller, G.D. *Plant Sociology; the Study of Plant Communities*, 1st ed.; Conard, H.S., Fuller, G.D., Eds.; McGraw-Hill Book Company, Inc.: New York, NY, USA; London, UK, 1932.
46. Dumelle, M.; Kincaid, T.; Olsen, A.R.; Weber, M. Spsurvey: Spatial Sampling Design and Analysis in R. *J. Stat. Softw.* **2023**, *105*, 1–29. [CrossRef] [PubMed]
47. Google LLC. Google Earth Pro (Version 7.1). 2024. Available online: https://www.google.it/intl/it/earth/versions/ (accessed on 5 January 2025).
48. Wood, S.N. *Generalized Additive Models*; Chapman and Hall/CRC: Boca Raton, FL, USA, 2017; ISBN 9781315370279.
49. Balestra, M.; Pierdicca, R.; Cesaretti, L.; Quattrini, G.; Mancini, A.; Galli, A.; Malinverni, E.S.; Casavecchia, S.; Pesaresi, S. A Comparison of pre-processing approaches for remotely sensed time series classification based on functional analysis. *ISPRS Ann. Photogramm. Remote Sens. Spat. Inf. Sci.* **2023**, *X-1/W1-2023*, 33–40. [CrossRef]
50. Pesaresi, S.; Mancini, A.; Quattrini, G.; Casavecchia, S. Evaluation and Selection of Multi-Spectral Indices to Classify Vegetation Using Multivariate Functional Principal Component Analysis. *Remote Sens.* **2024**, *16*, 1224. [CrossRef]
51. Younes, N.; Joyce, K.E.; Maier, S.W. All Models of Satellite-Derived Phenology Are Wrong, but Some Are Useful: A Case Study from Northern Australia. *Int. J. Appl. Earth Obs. Geoinf.* **2021**, *97*, 102285. [CrossRef]
52. European Space Agency SENTINEL-2 User Handbook. Available online: https://sentinel.esa.int/documents/247904/685211/Sentinel-2_User_Handbook (accessed on 26 November 2024).
53. Happ, C.; Greven, S. Multivariate Functional Principal Component Analysis for Data Observed on Different (Dimensional) Domains. *J. Am. Stat. Assoc.* **2018**, *113*, 649–659. [CrossRef]
54. Ramsay, J.O.; Silverman, B.W. (Eds.) *Functional Data Analysis*; Springer: New York, NY, USA, 2005; ISBN 9780387400808.
55. Levitin, D.J.; Nuzzo, R.L.; Vines, B.; Ramsay, J.O. Introduction to Functional Data Analysis. *Can. Psychol.* **2007**, *48*, 135–155. [CrossRef]
56. Marcinkowska-Ochtyra, A.; Gryguc, K.; Ochtyra, A.; Kopeć, D.; Jarocińska, A.; Sławik, Ł. Multitemporal Hyperspectral Data Fusion with Topographic Indices—Improving Classification of Natura 2000 Grassland Habitats. *Remote Sens.* **2019**, *11*, 2264. [CrossRef]
57. Tarquini, S.; Isola, I.; Favalli, M.; Mazzarini, F.; Bisson, M.; Pareschi, M.T.; Boschi, E. TINITALY/01: A New Triangular Irregular Network of Italy. *Ann. Geophys.* **2009**, *50*, 407–425. [CrossRef]
58. Breiman, L. Random Forest. *Mach. Learn.* **2001**, *45*, 5–32. [CrossRef]
59. Evans, J.S.; Cushman, S.A. Gradient Modeling of Conifer Species Using Random Forests. *Landsc. Ecol.* **2009**, *24*, 673–683. [CrossRef]
60. Congalton, R.G. A Review of Assessing the Accuracy of Classifications of Remotely Sensed Data. *Remote Sens. Environ.* **1991**, *37*, 35–46. [CrossRef]
61. Cohen, J. A Coefficient of Agreement for Nominal Scales. *Educ. Psychol. Meas.* **1960**, *20*, 37–46. [CrossRef]
62. Ranghetti, L.; Boschetti, M.; Nutini, F.; Busetto, L. "Sen2r": An R Toolbox for Automatically Downloading and Preprocessing Sentinel-2 Satellite Data. *Comput. Geosci.* **2020**, *139*, 104473. [CrossRef]
63. Hijmans, R.J. Raster: Geographic Data Analysis and Modeling. Available online: https://CRAN.R-project.org/package=raster (accessed on 4 December 2024).
64. Hyndman, R.J.; Khandakar, Y. Automatic Time Series Forecasting: The Forecast Package for R. *J. Stat. Softw.* **2008**, *26*, 1–22. [CrossRef]

65. Hyndman, R.; Athanasopoulos, G.; Bergmeir, C.; Caceres, G.; Chhay, L.; O'Hara-Wild, M.; Petropoulos, F.; Razbash, S.; Wang, E.; Yasmeen, F. Forecast: Forecasting Functions for Time Series and Linear Models. 2023. Available online: https://cran.r-project.org/web/packages/forecast/forecast.pdf (accessed on 5 January 2025).
66. Kuhn, M. Caret: Classification and Regression Training. Available online: https://CRAN.R-project.org/package=caret (accessed on 5 January 2025).
67. Vanden Borre, J.; Paelinckx, D.; Mücher, C.A.; Kooistra, L.; Haest, B.; De Blust, G.; Schmidt, A.M. Integrating Remote Sensing in Natura 2000 Habitat Monitoring: Prospects on the Way Forward. *J. Nat. Conserv.* **2011**, *19*, 116–125. [CrossRef]
68. Simonson, W.D.; Allen, H.D.; Coomes, D.A. Remotely Sensed Indicators of Forest Conservation Status: Case Study from a Natura 2000 Site in Southern Portugal. *Ecol. Indic.* **2013**, *24*, 636–647. [CrossRef]
69. Álvarez-Martínez, J.M.; Jiménez-Alfaro, B.; Barquín, J.; Ondiviela, B.; Recio, M.; Silió-Calzada, A.; Juanes, J.A. Modelling the Area of Occupancy of Habitat Types with Remote Sensing. *Methods Ecol. Evol.* **2018**, *9*, 580–593. [CrossRef]
70. Zlinszky, A.; Schroiff, A.; Kania, A.; Deák, B.; Mücke, W.; Vári, Á.; Székely, B.; Pfeifer, N. Categorizing Grassland Vegetation with Full-Waveform Airborne Laser Scanning: A Feasibility Study for Detecting Natura 2000 Habitat Types. *Remote Sens.* **2014**, *6*, 8056–8087. [CrossRef]
71. Questad, E.J.; Antill, M.; Liu, N.; Stavros, E.N.; Townsend, P.A.; Bonfield, S.; Schimel, D. A Camera-Based Method for Collecting Rapid Vegetation Data to Support Remote-Sensing Studies of Shrubland Biodiversity. *Remote Sens.* **2022**, *14*, 1933. [CrossRef]
72. Reckling, W.; Mitasova, H.; Wegmann, K.; Kauffman, G.; Reid, R. Efficient Drone-Based Rare Plant Monitoring Using a Species Distribution Model and Ai-Based Object Detection. *Drones* **2021**, *5*, 110. [CrossRef]
73. Swacha, G.; Botta-Dukát, Z.; Kącki, Z.; Pruchniewicz, D.; Żołnierz, L. A Performance Comparison of Sampling Methods in the Assessment of Species Composition Patterns and Environment–Vegetation Relationships in Species-Rich Grasslands. *Acta Soc. Bot. Pol.* **2017**, *86*. [CrossRef]
74. Pasquarella, V.J.; Holden, C.E.; Kaufman, L.; Woodcock, C.E. From Imagery to Ecology: Leveraging Time Series of All Available Landsat Observations to Map and Monitor Ecosystem State and Dynamics. *Remote Sens. Ecol. Conserv.* **2016**, *2*, 152–170. [CrossRef]
75. Zhu, X.; Liu, D. Accurate Mapping of Forest Types Using Dense Seasonal Landsat Time-Series. *ISPRS J. Photogramm. Remote Sens.* **2014**, *96*, 1–11. [CrossRef]
76. Barrett, B.; Raab, C.; Cawkwell, F.; Green, S. Upland Vegetation Mapping Using Random Forests with Optical and Radar Satellite Data. *Remote Sens. Ecol. Conserv.* **2016**, *2*, 212–231. [CrossRef] [PubMed]
77. Cabello, J.; Mairota, P.; Alcaraz-Segura, D.; Arenas-Castro, S.; Escribano, P.; Leitão, P.J.; Martínez-López, J.; Regos, A.; Requena-Mullor, J.M. Satellite Remote Sensing of Ecosystem Functions: Opportunities and Challenges for Reporting Obligations of the EU Habitat Directive. In Proceedings of the International Geoscience and Remote Sensing Symposium (IGARSS), Athens, Greece, 31 October 2018; pp. 6604–6607.
78. Corbane, C.; Lang, S.; Pipkins, K.; Alleaume, S.; Deshayes, M.; García Millán, V.E.; Strasser, T.; Vanden Borre, J.; Toon, S.; Michael, F. Remote Sensing for Mapping Natural Habitats and Their Conservation Status—New Opportunities and Challenges. *Int. J. Appl. Earth Obs. Geoinf.* **2015**, *37*, 7–16. [CrossRef]
79. European Parliament and Council Regulation (EU) 2024/1991 of the European Parliament and of the Council of 24 June 2024 on Nature Restoration and Amending Regulation (EU) 2022/869. 2024. Available online: https://eur-lex.europa.eu/eli/reg/2024/1991/oj/eng (accessed on 5 January 2025).
80. Bonanomi, G.; Caporaso, S.; Allegrezza, M. Effects of Nitrogen Enrichment, Plant Litter Removal and Cutting on a Species-rich Mediterranean Calcareous Grassland. *Plant Biosyst. An. Int. J. Deal. All Asp. Plant Biol.* **2009**, *143*, 443–455. [CrossRef]
81. Bonanomi, G.; Caporaso, S.; Allegrezza, M. Short-Term Effects of Nitrogen Enrichment, Litter Removal and Cutting on a Mediterranean Grassland. *Acta Oecologica* **2006**, *30*, 419–425. [CrossRef]
82. Catorci, A.; Cesaretti, S.; Gatti, R.; Ottaviani, G. Abiotic and Biotic Changes Due to Spread of *Brachypodium Genuense* (DC.) Roem. & Schult. in Sub-Mediterranean Meadows. *Community Ecol.* **2011**, *12*, 117–125. [CrossRef]
83. De Simone, W.; Allegrezza, M.; Frattaroli, A.R.; Montecchiari, S.; Tesei, G.; Zuccarello, V.; Di Musciano, M. From Remote Sensing to Species Distribution Modelling: An Integrated Workflow to Monitor Spreading Species in Key Grassland Habitats. *Remote Sens.* **2021**, *13*, 1904. [CrossRef]
84. Hurley, M.A.; Hebblewhite, M.; Gaillard, J.M.; Dray, S.; Taylor, K.A.; Smith, W.K.; Zager, P.; Bonenfant, C. Functional Analysis of Normalized Difference Vegetation Index Curves Reveals Overwinter Mule Deer Survival Is Driven by Both Spring and Autumn Phenology. *Philos. Trans. R. Soc. B Biol. Sci.* **2014**, *369*, 20130196. [CrossRef] [PubMed]
85. Pesaresi, S.; Mancini, A.; Casavecchia, S. Recognition and Characterization of Forest Plant Communities through Remote-Sensing NDVI Time Series. *Diversity* **2020**, *12*, 313. [CrossRef]
86. Müllerová, J.; Gago, X.; Bučas, M.; Company, J.; Estrany, J.; Fortesa, J.; Manfreda, S.; Michez, A.; Mokroš, M.; Paulus, G.; et al. Characterizing Vegetation Complexity with Unmanned Aerial Systems (UAS)—A Framework and Synthesis. *Ecol. Indic.* **2021**, *131*, 108156. [CrossRef]

87. Müllerová, J. UAS for Nature Conservation—Monitoring Invasive Species. In *Applications of Small Unmanned Aircraft Systems*; CRC Press: Boca Raton, FL, USA, 2019; pp. 157–178.
88. Zhou, H.; Zhu, J.; Li, J.; Xu, Y.; Li, Q.; Yan, E.; Zhao, S.; Xiong, Y.; Mo, D. Opening a New Era of Investigating Unreachable Cliff Flora Using Smart UAVs. *Remote Sens. Ecol. Conserv.* **2021**, *7*, 638–648. [CrossRef]
89. John, A.; Theobald, E.J.; Cristea, N.; Tan, A.; Hille Ris Lambers, J. Using Photographs and Deep Neural Networks to Understand Flowering Phenology and Diversity in Mountain Meadows. *Remote Sens. Ecol. Conserv.* **2024**, *10*, 480–499. [CrossRef]
90. Joly, A.; Goëau, H.; Bonnet, P.; Bakić, V.; Barbe, J.; Selmi, S.; Yahiaoui, I.; Carré, J.; Mouysset, E.; Molino, J.-F.; et al. Interactive Plant Identification Based on Social Image Data. *Ecol. Inform.* **2014**, *23*, 22–34. [CrossRef]
91. Kim, S.; Lee, C.W.; Park, H.J.; Lee, B.D.; Kim, N.Y.; Hwang, J.E.; Park, H.B.; An, J.; Baek, J.H. Piloting an Unmanned Aerial Vehicle to Explore the Floristic Variations of Inaccessible Cliffs along Island Coasts. *Drones* **2023**, *7*, 140. [CrossRef]
92. Soltani, S.; Ferlian, O.; Eisenhauer, N.; Feilhauer, H.; Kattenborn, T. From Simple Labels to Semantic Image Segmentation: Leveraging Citizen Science Plant Photographs for Tree Species Mapping in Drone Imagery. *Biogeosciences* **2024**, *21*, 2909–2935. [CrossRef]
93. Wang, L.; Zhang, M.; Gao, X.; Shi, W. Advances and Challenges in Deep Learning-Based Change Detection for Remote Sensing Images: A Review through Various Learning Paradigms. *Remote Sens.* **2024**, *16*, 804. [CrossRef]